Cleavage cracking across triple grain boundary junctions in freestanding silicon thin films

J. Chen and Y. Qiao[a)]
Department of Structural Engineering, University of California—San Diego, La Jolla, California 92093-0085

(Received 28 October 2007; accepted 20 February 2008)

This article is focused on a fractography study of cleavage cracking at triple grain boundary junctions in freestanding silicon thin films. At a triple junction, as the crystallographic orientations of the two grains ahead of the crack are different by only a few degrees, the cleavage front advance becomes quite jerky. The crack first enters the grain of smaller boundary toughness and then turns into the other grain from the lateral direction. Consequently, the overall fracture resistance cannot be analyzed in the framework of line-average theory. The nonuniform characteristic of crack behavior can be attributed to the increase in local stress intensity. A few typical crack front advance modes are identified.

I. INTRODUCTION

Understanding fracture behaviors of polycrystalline thin films is of great importance to assuring safe performance of micro/nanoelectromechanical systems, integrated circuits, sensors, etc.[1] During film growth, if the substrate temperature T_{sub} is relatively high, the grains are equiaxed; if T_{sub} is relatively low, because of the difficulty in surface diffusion, the grain structure becomes columnar.[2] The growth rate of a grain is highly dependent on its orientation. For instance, in a low-temperature chemical vapor deposition process, $\langle 110 \rangle$ is the most prevalent out-of-plane direction for silicon.[3,4] As a result, as the film becomes thicker, the growth of nuclei of unfavorable orientations is interrupted, and the microstructure is dominated by the grains that can eventually become large.[5] The fracture toughness of such a film is governed by the through-thickness grain boundaries.[6] If the film is relatively thin, e.g., when the film thickness is only a few micrometers, the influence of buried grains can be significant, as their sizes are comparable with film thickness. When a cleavage front propagates across these boundaries, it must overcome triple junctions, which can have considerable effects on the size dependence of fracture and failure mechanisms and processes at small length scales[7–10] as well as the grain boundary behaviors.[11,12]

There are a few possible cleavage cracking modes at a triple grain boundary junction. It is sometimes assumed that the crack can simultaneously enter the two grains ahead of the front. The overall resistance offered by the triple junction can then be taken as the average of the fracture resistances of the two boundaries.[13,14] Another possible crack advance mode is postponed propagation.[15] The crack front would first break through the boundary of lower resistance, and the rest is arrested by the one that is of higher resistance. At the protruding section (the convex part) of the front, the local stress intensity is smaller than that at the concave part (the section that is left behind). The latter would eventually overcome the boundary, and the front tends to be straight again. Under this condition, the overall fracture resistance can still be analyzed in the framework of line average theory, with the contributions of the boundary between the two grains being taken into consideration.[16] Such analyses can provide quite accurate predictions for fracture resistances of bulk polycrystalline materials,[17] since when a cleavage crack propagates across a field of grains, the fracture work is determined by the contributions from all the grains encountered by the front, and the fluctuation in local resistance can be averaged out. In a thin film material, however, along the entire crack front there are only a small number of grains, and therefore the chronology of front advance must be taken into account. According to the fracture experiment on silicon thin films, which will be discussed shortly, in the samples under investigation, neither the simultaneous break-through mode nor the postponed propagation mode was observed. The crack front always entered one grain first and then turned into the other from the lateral direction.

II. EXPERIMENTAL

Figure 1 depicts the sample structure. As the tensile load is increased gradually, the transmission process of a

[a)]Address all correspondence to this author.
e-mail: yqiao@ucsd.edu
DOI: 10.1557/JMR.2008.0206

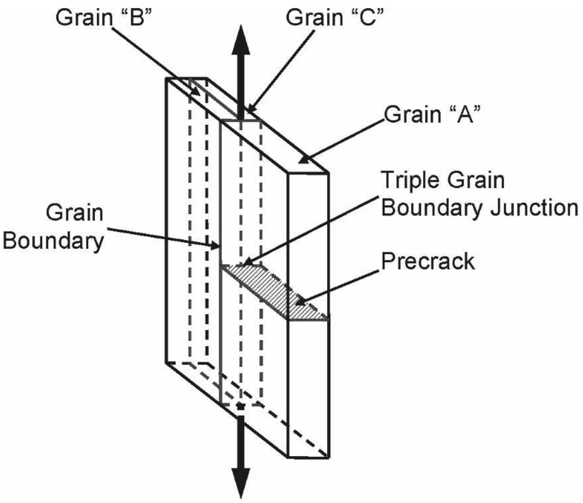

FIG. 1. Schematic illustration of a free-standing thin film sample with a triple grain boundary junction.

cleavage front from the grain behind the junction (A) to the two grains ahead of it (B and C) can be examined. In the current study, we investigated polycrystalline silicon with grain size of about 10 mm. The as-received material was in wafer form, 4 mm thick. The silicon was heavily doped by boron. The precrack was produced through a controlled-quenching process. The wafer was first heated to 450 °C, and then one half of it was immersed in cold water. Because of the steep temperature gradient, a large number of thermal cracks were generated, many of which were arrested by grain boundaries. The thermal cracks became clearly visible after the wafer was etched for a few minutes in a dilute hydrofluoric acid etchant. At each side of the wafer, the orientations of the grains could be analyzed through Laue x-ray backscatter measurement. The cracks that were arrested by different grains at both sides of the wafer were identified. Along the front of such a crack, there was at least one triple grain boundary junction.

Silicon blocks (15 mm × 15 mm) that contained suitable crack tips were harvested from the wafer by electrical discharge machining (EDM). They were then EDM cut along the crack direction into 0.2-mm-thick slides and mechanically polished down to about 100 μm. To further reduce film thickness and protect precrack surfaces, hydroxyl groups were end-capped by silane groups. The surface-modification process was similar to that of nanoporous silicas,[18] except that the treatment time (120 h) was much longer. The treated surfaces were highly hydrophobic, and therefore when the sample was immersed in etchant, the precrack surface would not be affected. After the silane groups on the sample surfaces were removed by mechanically polishing, the sample was thinned by critical etching to about 10–15 μm. The etchant contained 7% of hydrofluoric acid, 75% of nitric acid, and 18% of acetic acid. During etching, the etchant flowed across the sample surface at a constant rate of 30 mL/min. The flow was controlled by an Omega peristaltic pump. The film thickness was examined every 3–5 min using a laser interferometer. The etching rate was 3–5 μm/min.

The thin-film sample was mounted on the sample stage of a microtensile machine by using Loctite-411 glue. The design and characterization of the testing machine were described in a previous work.[19] By using an inchworm actuator, a tensile load normal to the precrack plane was applied. As the crossheads moved apart at the rate of 10 μm/s, the precrack would eventually overcome the triple junction. Figures 2–5 show typical scanning electron microscope (SEM) images of fracture surfaces.

III. RESULTS AND DISCUSSION

The orientations of the two grains ahead of the triple boundary junction in the samples under investigation distribute quite randomly. The twist misorientation angle was in the range of 6°–24°, and the tilt misorientation angle was in the range of 5°–19°. Note that in silicon because cleavage cracking can occur along both {110} and {111} planes, usually the misorientation angles of cleavage surfaces across a grain boundary are less than 25°. In all the cases, simultaneous break-through of cleavage front across the two boundaries between grains A and B and A and C never takes place. The crack front always penetrates first through the boundary of the smaller twist misorientation angle, as shown in Fig. 2. Initially, the precrack front is aligned along the boundaries at both sides of the triple junction. As the external tensile load increases, the local stress intensity along the front $K(x)$ rises gradually, where x indicates the axis normal to the crack advance direction. Since the front is straight, $K(x)$ should be quite uniform, and therefore the crack would penetrate through the boundary where the local fracture resistance is lower. According to a previous

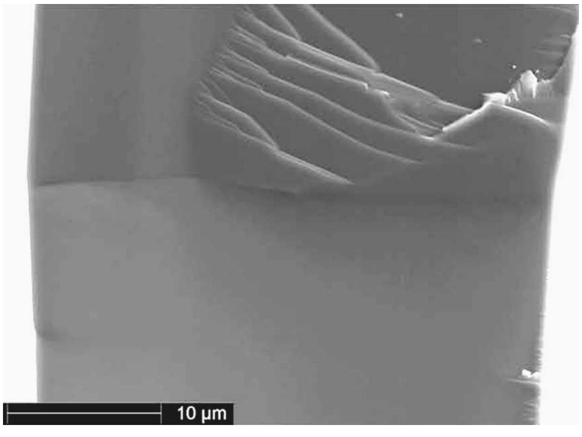

FIG. 2. SEM image of a cleavage crack turning around a triple junction. The crack propagates from the bottom to the top.

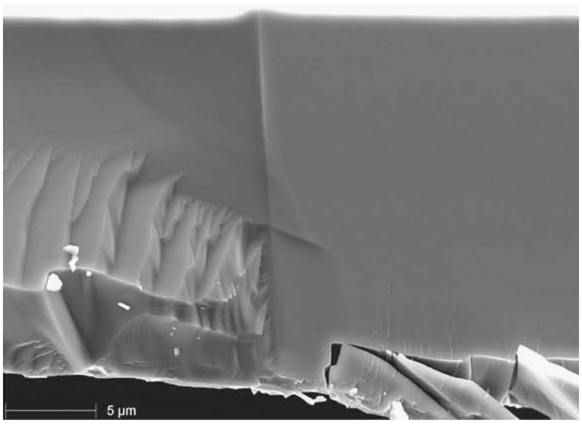

FIG. 3. SEM image of a cleavage crack entering a grain from both sides. The crack propagates from the right to the left.

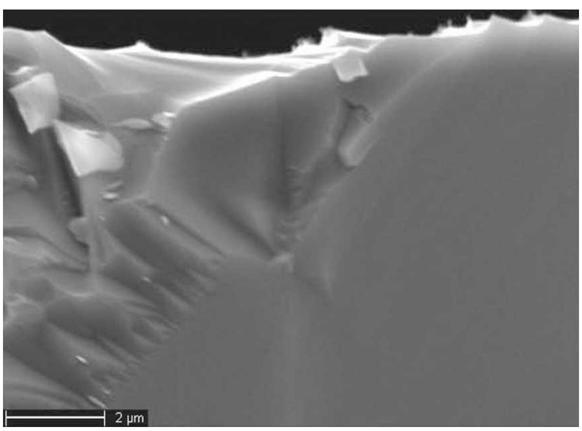

FIG. 4. SEM image of a cleavage crack entering back into the grain behind the boundary. The crack propagates from the left to the right.

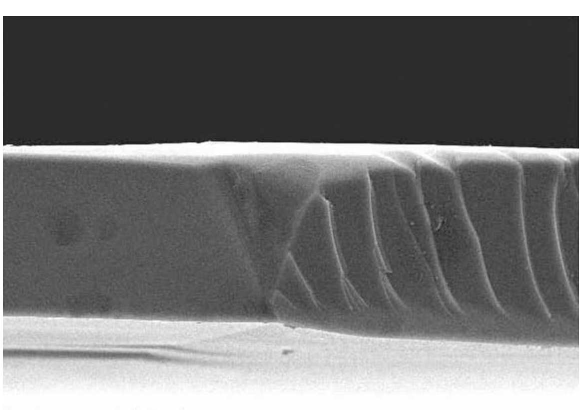

FIG. 5. SEM image of a cleavage crack bypassing a relatively small grain. The crack propagates from the right to the left.

analysis,[20] the relationship between crystallographic orientation and boundary toughness is

$$K_{GB}/K_{SC} = \sqrt{(\sin\theta + \cos\theta)/\cos^2\phi + C_0 \cdot \sin 2\theta/\cos\phi} \quad , \qquad (1)$$

where θ and ϕ are twist and tilt angles, respectively, K_{SC} is the effective toughness of a crystallographic plane, and C_0 is a material constant. As θ or ϕ increases, K_{GB} becomes larger, and the effect of θ is more pronounced; that is, it is likely that the boundary with smaller twist angle is of a lower fracture resistance, which is compatible with the experimental observation.

Once the crack penetrates into one of the grains (B), there are at least two possible ways for its front to enter the other one (C). The first is the postponed propagation that has been discussed previously. The front sections left behind the verge of propagating front would overcome the barrier effect of the boundary between grains A and C, and advances faster than the front section in grain B, so that the entire front tends to be straight again. However, this mode was not observed in our experiment. The other possible mechanism, as depicted in Fig. 6, is kink-type propagation, which occurs in all the thin-film samples. After the front enters grain B, a kink-type structure would be formed in the cleavage front, connecting together the protruding part and the arrested part. As the advance distance in grain B is relatively large, the kink-type front section would overcome the boundary between grains B and C, entering grain C from the lateral direction, and thus the separation of the entire fracture surface around the triple junction is completed. Such a front behavior is somewhat similar to the propagation of a half double-kink along a screw dislocation.[21]

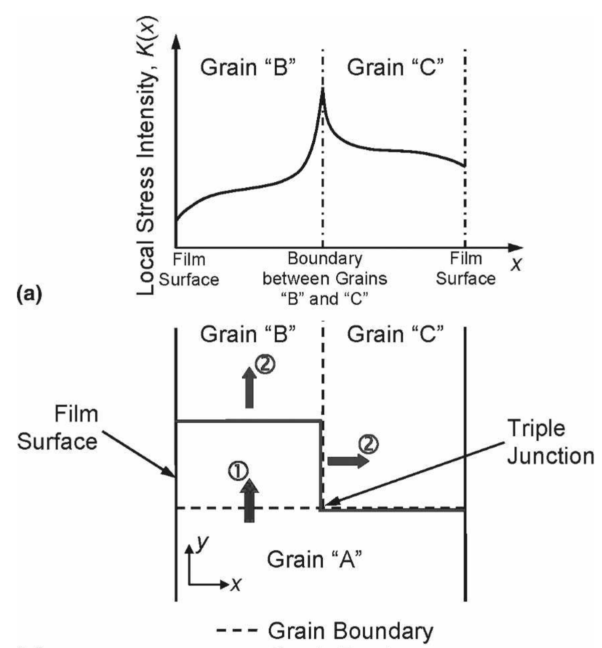

FIG. 6. Schematic illustrations of (a) the local stress intensity and (b) the front profile of a cleavage crack propagating across a triple grain boundary junction. Arrow ① indicates the front propagation across the boundary between grains A and B; arrows marked ② indicate the front behaviors inside grain B and across the boundary between grains B and C.

In the sample shown in Fig. 2, the twist angle of the boundary between the two grains ahead of the triple junction was 14°; the twist angels of the other two boundaries were 6° and 11°, respectively. The measured grain boundary toughness was 1.90 MPa $m^{1/2}$. The crack front first overcame the boundary of the twist angle of 6°, entering from grain A to B. Then, instead of breaking through the boundary of the twist angle of 11°, it propagated into the third grain (C). This should be attributed to the nonuniform distribution of local stress intensity. As shown in Fig. 6(a), through either perturbation analysis[22–24] or numerical simulation,[25] it has been well known that the stress field at a crack tip is highly dependent on the front profile. At the verge of propagating front, the local stress intensity is smaller, and along the front section that is left behind, the local stress intensity is higher. The value of $K(x)$ near a free surface tends to be lower. Most importantly, a peak of $K(x)$ can be formed at a corner, e.g., a kink section. If the corner is perfectly sharp, the local stress intensity tends toward infinity. Therefore, even if the local fracture resistance is slightly higher, once the kink-type structure is formed, the front would expand at the location where the local $K(x)$ reaches the maximum value.

In Fig. 3, with respect to the initial crack surface, the twist angle of the upper grain ahead of the triple junction was 8°, and that of the bottom one was 11°, only slightly different. The twist angle at the boundary between the two grains was 16°. The measured grain boundary toughness was 1.95 MPa $m^{1/2}$. It can be seen that the crack front enters the bottom grain along two directions from both the upper grain and the grain behind the triple junction. However, it is clear that the break-through of the boundary between the two grains ahead of the triple junction happens first, which dominates the separation of fracture surfaces. Only when most of the bottom grain has cracked does the arrested front section start to advance.

One interesting phenomenon is that the break-through modes along the boundary exposed to the initial crack front and the lateral boundary between the two grains ahead of the triple junction are quite different. As shown in Fig. 2, when the front bypasses the boundary between grains A and B, very often there is only one break-through point; i.e., the front first penetrates through the boundary at a single point, and once the penetration depth is relatively large the entire boundary is separated apart. At the boundary between grains B and C, the front penetrates through the boundary at a number of points. The fracture surface shifts from the cleavage plane of grain B to that of grain C locally, forming a series of parallel terraces. The cleavage front breaks down into many segments; each segment advances quite independently, until secondary fracture takes place and these terraces are connected. The edges of the terraces become river markings. It should be related to the intrinsic distance between break-through points w. At the boundary between grains A and B, w is relatively large, and along the entire boundary there is only one break-through point. At the boundary between grains B and C, w is considerably smaller, and thus a number of break-through points can be formed. The factors that govern the break-through-point distance are still under investigation. They probably include the dynamic effect, the mixed fracture mode, the variation in local crack growth driving force, and/or the chronology of front motion. For instance, as the front propagates further in grain B, it is likely that it may branches into grain C quasi-periodically.

In some cases, the arrested crack front section never breaks through the tougher boundary, even after the fracture surfaces are completely separated. In Fig. 4, the cleavage front first enters the bottom grain ahead of the triple junction and then breaks through the lateral boundary and advances into the upper grain. Instead of shearing apart the persistent grain boundary, the front goes back from the upper grain to the grain behind the triple junction. That is, a few break-through points are formed as the front penetrates across the boundary locally. When the front segments merge, an undercut is created. In Fig. 5, since the upper grain exposed to the initial crack front is quite small, once the front enters the bottom grain it entirely surrounds the upper one, cracking it from the far end.

IV. CONCLUSION

To summarize, through a fractography study, the cleavage cracking processes across triple grain junctions in silicon thin films were investigated. The crack front bypasses triple junction nonuniformly, somewhat similar to the kink motion along a dislocation line. It first breaks through the grain boundary of lower resistance, and then enters the other grain from the lateral direction, which can be related to the local stress concentration at the kink-type front section. Thus, the overall fracture resistance of the triple junction should not be assessed by using line-average theory. The failure modes at the boundary exposed to the initial crack front and the lateral boundary are quite different.

ACKNOWLEDGMENT

This work was supported by the United States Department of Energy, Office of Basic Energy Sciences under Contract No. DE-FG02-07ER46355.

REFERENCES

1. M. Ohring: *The Materials Science of Thin Films* (Academic Press, Oxford, UK, 1992).

2. C.V. Thompson: Structure evolution during processing of polycrystalline films. *Ann. Rev. Mater. Sci.* **30,** 159 (2000).
3. T.I. Kamins: Structure and properties of LPCVD silicon films. *J. Electrochem. Soc.* **127,** 686 (1980).
4. P. Joubert, M. Sarret, L. Haji, L. Hamedi, and B. Loisel: Pressure dependence of in situ boron doped silicon films prepared by low-pressure chemical vapor deposition I. *Microstruct. J. Appl. Phys.* **66,** 4806 (1989).
5. D.J.J. Srolovitz: Grain growth phenomena in films—A Monte Carlo approach. *Vac. Sci. Technol., A* **4,** 2925 (1986).
6. Y. Qiao and X. Kong: On size effect of cleavage cracking in polycrystalline thin films. *Mech. Mater.* **39,** 746 (2007).
7. J.L. Wang, J. Lian, J.R. Greer, W.D. Nix, and K.S. Kim: Size effect in contact compression of nano- and micro-scale pyramid structures. *Acta Mater.* **54,** 3973 (2006).
8. J.R. Greer, W.C. Oliver, and W.D. Nix: Size dependence of mechanical properties of gold at the micro scale in the absence of strain gradients. *Acta Mater.* **53,** 1821 (2005).
9. G. Feng and W.D. Nix: Indentation size effect in MgO. *Scripta Mater.* **51,** 599 (2004).
10. J. Marian and J. Knap: Breakdown of self-similar hardening behavior in Au nanopillar microplasticity. *Int. J. Multiscale Comput. Eng.* **5,** 287 (2007).
11. D.H. Choi, H. Kim, and W.D. Nix: Anelasticity and damping of thin aluminum films on silicon substrates. *J. MEMS* **13,** 230 (2004).
12. V.V. Beloulsov: Surface ionics: A brief review. *J. Euro. Ceramic Soc.* **27,** 3459 (2007).
13. J. Lin, Y. Liu, and T.A. Dean: A review on damage mechanisms, models, and calibration methods under various deformation conditions. *Int. J. Damage Mech.* **14,** 299 (2005).
14. I.A. Ovid'ko: Review on the fracture processes in nanocrystaline materials. *J. Mater. Sci.* **42,** 1694 (2007).
15. A. Crocker, G. Smith, P. Flewitt, and R. Moskovic: Grain boundary fracture in the cleavage regime of polycrystalline materials, in *Proc. 11th European Conf. on Fracture* (Eng. Mater. Advis. Serv. Warley, UK, 1996), p. 233.
16. Y. Qiao and X. Kong: Cleavage resistance of fine-structured materials. *Met. Mater. Inter.* **12,** 27 (2006).
17. Y. Qiao and A.S. Argon: Cleavage crack-growth-resistance of grain boundaries in polycrystalline Fe–2 wt% Si alloy. *Mech. Mater.* **35,** 129 (2003).
18. A. Han and Y. Qiao: Controlling infiltration pressure of a nanoporous silica gel via surface treatment. *Chem. Lett. (Jpn.)* **36,** 882 (2007).
19. Y. Qiao, E. Pan, S.S. Chakravarthula, F. Han, J. Liang, and S. Gudlavalleti: Measurement of mechanical properties of rectal wall. *J. Mater. Sci.: Mater. Med.* **16,** 183 (2005).
20. Y. Qiao and A.S. Argon: Cleavage cracking resistance of high angle grain boundaries in Fe–3 wt% Si alloy. *Mech. Mater.* **35,** 313 (2003).
21. B.J. Gally and A.S. Argon: Brittle to ductile transitions in the fracture of silicon single crystals by dynamic crack arrest. *Philos. Mag.* **81,** 699 (2001).
22. L.R.F. Rose: Toughening due to crack front interaction with a 2nd-phase dispersion. *Mech. Mater.* **6,** 11 (1987).
23. H. Gao and J.R. Rice: Application of 3D weight functions. 2. The stress field and energy of a shear dislocation loop at a crack tip. *J. Mech. Phys. Solids* **37,** 155 (1989).
24. X. Kong and Y. Qiao: Fracture in ceramic-matrix composites reinforced with strongly bonded metal particles. *Mech. Compos. Mater.* **41,** 205 (2005).
25. G. Xu, A.F. Bower, and M. Ortiz: The influence of crack trapping on the toughness of fiber reinforced composites. *J. Mech. Phys. Solids* **46,** 1815 (1998).